

# **Seismic Fragility of Italian RC Precast Industrial Structures**

C. Casotto<sup>1</sup>\*, V. Silva<sup>2</sup>, H. Crowley<sup>2</sup>, R. Nascimbene<sup>2</sup>, R. Pinho<sup>3</sup>

<sup>1</sup>*ROSE Programme, UME School, IUSS Pavia, Italy*

<sup>2</sup>*European Centre for Training and Research in Earthquake Engineering (EUCENTRE), Pavia, Italy*

<sup>3</sup>*Department of Civil Engineering and Architecture, University of Pavia, Italy*

## **ABSTRACT**

Despite the moderate ground motions observed during the seismic events in Northern Italy, May 2012, reinforced concrete (RC) precast industrial buildings suffered excessive damage, which led to substantial direct and indirect losses. The aim of this paper is to present a seismic fragility model for Italian RC precast buildings, to be used in earthquake loss estimation and seismic risk assessment. An analytical methodology has been used that consists of 1) random sampling of one hundred structures for each building typology, 2) pushover analysis to establish a number of damage limit states, 3) execution of nonlinear dynamic analysis and comparison of the maximum demand with the limit state capacity to allocate the structure in a damage state, and 4) regression analysis on the cumulative percentage of buildings in each damage state for a set of intensity measure levels to derive the statistical parameters of the fragility functions. The building population employed in the analysis was generated considering both material and geometric variability that was obtained from the field surveys of 650 industrial facilities, as well as other information available in the literature. Several aspects of the fragility derivation process were further analysed, such as the correlation between different intensity measure types and damage, the consideration of different collapse mechanisms (e.g. beam-column connection failure) and the differences in the resulting fragility curves when adopting a 2D or a 3D modelling environment. A good agreement with preliminary empirical fragility functions based on field data was also observed.

*Keywords:* seismic fragility, RC precast structures, 2D and 3D modelling, beam-column connection collapse

## **1 INTRODUCTION**

Seismic fragility is a measure of the likelihood of a building suffering damage for a given severity of ground shaking, and it can be mathematically formulated by fragility curves, which describe the probability of reaching or exceeding a certain damage limit state for a given intensity of ground motion. Fragility models have been developed mostly for residential buildings, and there are few capable of characterising the seismic behaviour of reinforced concrete (RC) precast structures, notwithstanding the damage often observed in

---

\* Corresponding author.

*E-mail address:* chiara.casotto@umeschool.it

these structures during moderate earthquakes, and the associated direct and indirect consequences in terms of both human casualties, as well as economic losses due to business interruption.

In May 2012, the seismic events in Northern Italy revealed the seismic vulnerability of typical Italian precast industrial buildings. These structures are frequently more flexible than traditional reinforced concrete frames due to their structural scheme, which is composed of cantilevered columns fixed at the base and a high inter-storey height. The connections between precast beams and columns, and between roof elements and beams should be able to sustain the seismic displacement demand associated with the structure's high flexibility, but are often designed only to transfer horizontal forces by friction or through steel dowels. Figure 1.1 demonstrates how the use of these connections has led to the loss of support of the structural elements, and consequently to their collapse, in the aforementioned recent events.



**Figure 1.1 Failure due to loss of support of the beam during the May 2012 Emilia-Romagna earthquake in Northern Italy [Belleri et al. [1]].**

The poor seismic behaviour of these structures during the May 2012 event in Northern Italy is mainly due to the fact that the first seismic design regulation for this typology was introduced in Italy only in 1987 and a seismic hazard zonation of the Italian territory that adequately considered the hazard in this part of the country was released only in 2004. As a consequence, a large number of structures were designed before the enforcement of the more recent seismic regulations, and thus exhibit a number of structural deficiencies (Belleri et al. [1]). The aforementioned deficiencies affect strongly the response of precast industrial buildings to seismic excitation, as compared to traditional cast-in-place RC structures, and for this reason this paper investigates whether the inevitably necessary simplifications in the modelling and methodologies used to derive fragility curves still allow the effects of such design deficiencies to be captured.

Several methodologies have been proposed in the recent decades for the derivation of damage-ground motion intensity relationships, as summarised by Calvi et al. [2]. These include the statistical treatment of damage distributions that have either been observed in post-earthquake surveys (empirical relationships) or simulated through structural analyses of numerical models under increasing earthquake intensity (analytical relationships). The latter approach allows sensitivity studies to be carried out to evaluate the impact of specific aspects, such as inadequate detailing, on the overall structural response. In addition, analytical approaches permit the vulnerability assessment of classes of buildings for which reliable statistical damage data might not be available. For this reason, an analytical method was used in the seismic fragility study presented herein.

One of the main differences between the various analytical methods arises in the procedure used to estimate the nonlinear response of the structure for a given ground motion input. The computational efficiency of

static analysis with respect to dynamic analysis has triggered the development of many Nonlinear Static Procedures, in which the seismic capacity of the structure is usually represented by a capacity curve and the seismic demand by an acceleration and/or displacement response spectrum. For example Borzi et al. [3] developed a Simplified Pushover-based Earthquake Loss Assessment method (SP-BELA), where the nonlinear behaviour of a random population of buildings is defined through a simplified pushover curve, and the fragility curves are generated through the comparison between the displacement capacity limits identified on the pushover curve and the displacement demand from a response spectrum. Bolognini et al. [4] implemented the SP-BELA method for traditional Italian precast constructions, adapting the limit states definition and considering the connection failure mechanism in a simplified way that ignored the vertical component of the dynamic seismic input. Senel and Kayhan [5] have also derived fragility curves for precast industrial buildings also using simplified pushover curves for the definition of the limit states, expressed as a function of the chord rotation of the columns. However, in this case, nonlinear dynamic analyses were employed to obtain the maximum displacement demands, which were compared with the aforementioned limit displacements. The main drawbacks of this fragility assessment are the exclusion of the second order effects in the mechanics-based bilinear pushover curves, which in this type of structures can affect considerably the overall behaviour, and the lack of modelling of the connection behaviour.

For what concerns nonlinear dynamic analysis, in general the two most common disadvantages to its use in fragility assessment are the increased computational effort and the difficulty in readily guaranteeing numerical convergence. However, such issues were not a main concern within this study as the structures under investigation are relatively simple (single-storey bare frames), which thus allowed the employment of a large number of nonlinear dynamic analyses and a more accurate representation of the real phenomenon. Hundreds of structures were produced through Monte Carlo simulation to represent the “as built” in Italy and subjected to seventy ground motion records using nonlinear dynamic analysis. The geometric properties of the structures generated were randomly sampled from probabilistic distributions obtained from 650 field surveys, while the material property distributions were found in the literature and established using expert opinion, when such data were not available. The building stock was classified into a number of typologies according to geometric configuration and the original seismic design, both of which are correlated with the construction age. This methodology was implemented by modelling the structures in both 2D and 3D frameworks. A pushover analysis was also performed for each frame and a set of limit states were estimated according both to strain levels and maximum top drifts. The capacity of the connections was calculated and connection failure was accounted for as a collapse limit state, estimated with both static and dynamic methods.

## **2 FRAGILITY CURVE METHODOLOGY**

An overview of the analytical methodology for the derivation of the fragility curves is shown in Figure 2.1. The analytical methodology can be summarised in the following steps:

1. *Generation of precast RC structures*: The characteristics of this type of structure were analysed according to building typologies with homogeneous attributes. For each typology, a probability density function for each geometric and material parameter was defined.
2. *Design, numerical modelling and damage analyses*: The randomly sampled single structures were designed according to the admissible tension method and the provisions of the code in place at the time of construction (either pre- or post-1996). The classification of the building stock and the design procedure outlined by Bolognini et al. [4] was adopted. Each generated structure was modelled and subjected to nonlinear static and dynamic analyses using the software OpenSEES [1]. The pushover analysis served the purpose of defining a capacity curve, and the associated limit states

(LSs) for three levels of damage. Due to the particular static scheme and the structural deficiencies affecting the nonlinear behaviour of precast RC buildings, both sectional and global parameters were used for the limit state definition. The steel yielding strain characterises the first limit state and the maximum top drift defines the collapse limit state, unless connection failure happens first. A dynamic analysis was performed using a suite of selected accelerograms and the maximum response of each structure in terms of maximum top drift was extracted. These results (displacement demand) were compared with the limit states (displacement capacity), in order to allocate each structure into a damage state.

3. *Fragility curves derivation*: The distribution of buildings in each damage state was stored in a damage probability matrix (DPM), and related to the corresponding Intensity Measure Level (IML) for each ground motion record (described further in Section 2.3). The DPM was used to derive the statistical parameters of each fragility function. This regression analysis was carried out using the maximum likelihood method.

## 2.1 Generation of the building stock

A Matlab [2] script was developed to incorporate the different steps of the analysis presented in Figure 2.1 into an automated process.

### *Classification of Italian industrial precast buildings*

The definition of the typologies representative of the “as built” in Italy was based on the combination of different factors: the year of construction and thus the seismic design code to which they should conform to, and the geometric configuration. A period corresponding to the last 50-60 years was considered and the building stock subdivided between pre-code and low-code design, for the structures that date back to before and after 1996, respectively. In fact the first (unsatisfactory) attempts to include provisions for the design of reinforced concrete precast structures in seismic zones were carried out in 1987 and 1996, but an appropriate design code including a specific chapter on precast structures was introduced only in 2003 (OPCM 3274 [6]). The very limited number of precast buildings in Italy designed in accordance with the latter regulation meant that it was not worth considering a post-code typology with modern seismic design in the adopted classification. Moreover, the little knowledge of the real design criteria applied in the absence of code provisions in the decades before the ‘70s, combined with the relatively scarce design documentation, results in a large uncertainty in the evaluation of the capacity of RC precast structures built in that period.

Two main categories were selected to represent the most common geometric configurations of the Italian precast industrial building stock, as described in Table 2.1. This classification was developed based on information from the available Italian literature, from precast elements producers, and designs reported in Calvi et al. [7, 8], and from the direct survey of 650 warehouses located in Tuscany, Emilia Romagna and Piedmont regions, built between 1960 and 2010. Part of the survey data were provided by the Seismic Risk Prevention Area of Tuscany Region [3], which conducted a campaign for risk and hazard assessment of industrial areas, which is fully described in Ferrini et al. [9]. Additional information was collected by field teams from the European Centre for Training and Research in Earthquake Engineering [4]. The results of the investigations were used to derive the statistical distributions of the geometric properties for each building typology. Some information required for this study (e.g. material properties and design loads) could not be extracted from the surveys, and was instead obtained from the literature, or estimated through expert opinion.

The first typology, more traditional and frequently used, consists of a series of one-storey basic portal frames. Each portal is comprised of two or more columns fixed at the base and a saddle roof beam, usually simply supported by the columns or with shear resistant connections. The second common typology consists

of one-storey frames linked by perpendicular straight beams, which carry the main roof beams or directly support the large span slab elements. Table 2.1 describes the classification of the building stock according to the structural configuration and the design lateral load.

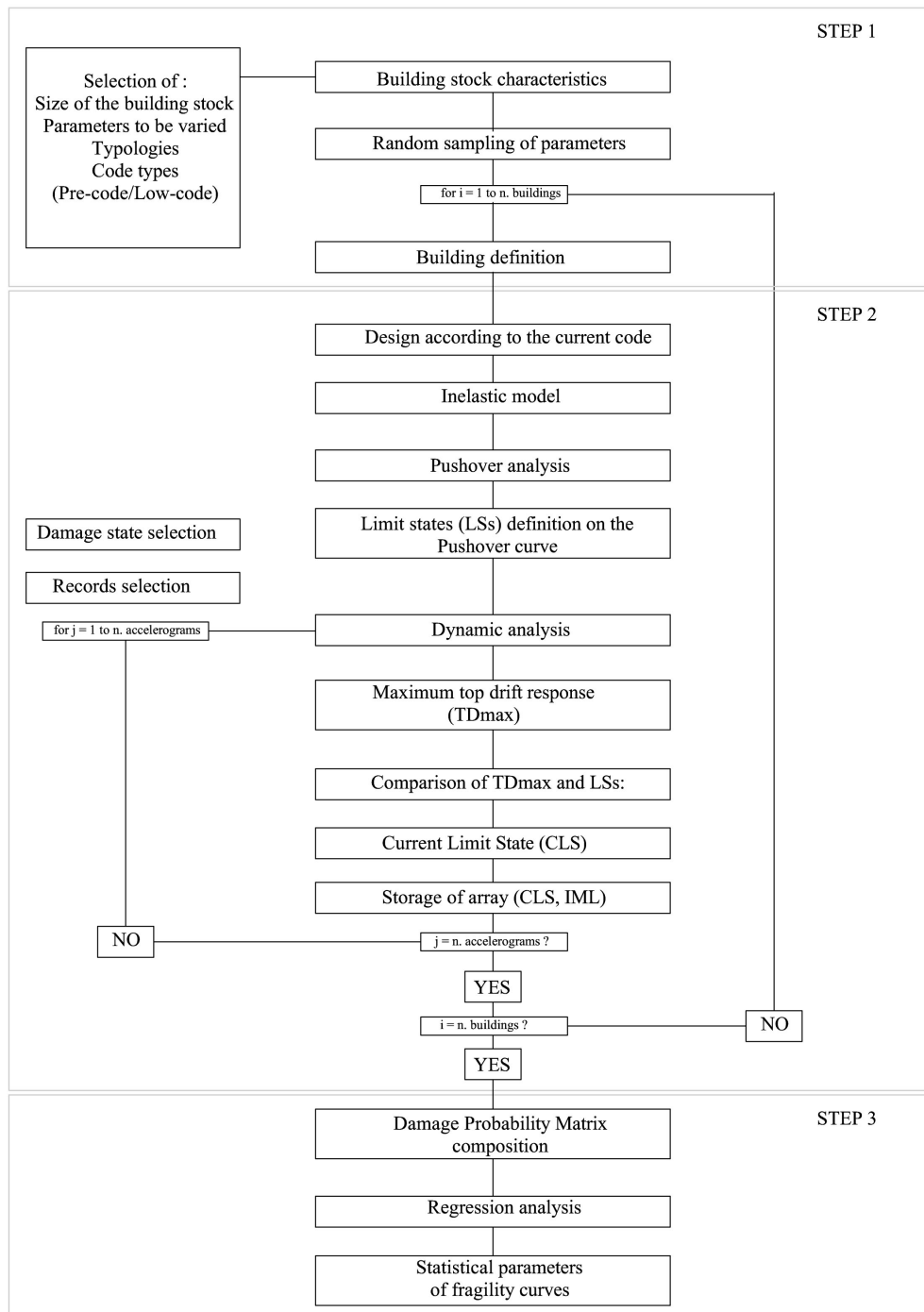


**Figure 2.1 Flowchart of the proposed analytical method to derive fragility curves**

**Table 2.1 Classification of the building typologies used in this study.**

Structural configuration	Code level	Design lateral load*	Id code
 <p>Type 1</p>	Pre-code	2%	T1-PC-2
	Low-code	4%	T1-LC-4
		7%	T1-LC-7
		10%	T1-LC-10
 <p>Type 2</p>	Pre-code	2%	T2-PC-2
	Low-code	4%	T2-LC-4
		7%	T2-LC-7
		10%	T2-LC-10

\* as a percentage of the weight of the structures

### ***Statistical characterization of the material and geometric parameters***

The concrete and steel characteristic compressive and tensile strengths were sampled according to the construction age. The material properties indicated by the reference codes (DM 3-03-1975 [10], DM 16-01-1996 [11]) were used to design each structure. For the design of the low-code typologies a random choice between the steel characteristic yielding value of 380 MPa and 440 MPa was performed, which corresponds to the values indicated by the DM 16-01-1996 [11] regulation for FeB38 and FeB44 ribbed steel bars, respectively. The same approach was adopted for the concrete cubic characteristic strength, with randomly selected values of 45, 50 or 55 MPa (each with the same probability of occurrence). For the pre-code typologies, values between 320 MPa and 380 MPa were randomly chosen for steel tensile strength, according to the DM 3-03-1975 [10] guidelines, the former referring to FeB32 smooth bars and the latter to the FeB38 ribbed bars. Regarding the concrete compressive strength for this typology, 35, 40, 45 or 50 MPa was randomly chosen from a uniform distribution. Both smooth and ribbed steel bars were considered in the pre-code classification because of the progressive increase in the use of ribbed bars, passing from 5% in 1950 to 80% in 1980 (Verderame et al. [12]).

In order to consider the difference between the actual characteristic compressive and tensile strength of the materials to be used in the modelling and the design values indicated in the codes, the results obtained by Verderame et al. [12] from an experimental campaign on the actual mechanical properties of materials were adopted. Unfortunately, this study provides information only on smooth steel bars, hence overstrength coefficients to the design values of those materials for which statistical studies were not available were applied. Therefore, a normal distribution with a mean of 356 MPa and standard deviation of 67.8 MPa was assumed for the steel yielding strength of smooth bars (Verderame et al., [12]), while the yielding strength of ribbed bars and the characteristic strength of concrete were respectively multiplied by the overstrength coefficients  $\gamma_s$  (mean value of 1.15 and coefficient of variation equal to 7.5%) and  $\gamma_c$  (mean value of 1.3 and coefficient of variation equal to 15%), following the suggestions of Bolognini et al. [4]. It is noted that for the modelling, the overstrength coefficients were not applied to the same design values adopted in the design, but to new randomly sampled design values. In fact, the characteristic strengths used in the design are generally unknown when trying to assess the capacity of an existing building; the new sampling thus takes into account the possible mismatch between the design and the modelling values, which is another source of uncertainty.

Table 2.2 summarises concrete and steel characteristic strengths ( $R_{ck}$  and  $f_{sk}$ ) used for the design and Table 2.3 provides the values used in the modelling. Table 2.4 reports the loads applied in the simulated design: the self-weight of the roof  $G_R$  and the beam  $G_B$  are a function of the length that the roof elements and the beams need to cover,  $L_{intercol}$  and  $L_{beam}$ , respectively.

**Table 2.2 Material properties randomly sampled for the simulated design of the building stock.**

	Pre-code (all cases)	Low-code (all cases)
$R_{ck}$ [MPa]	35, 40, 45, 50	45, 50, 55
$f_{sk}$ [MPa]	320, 380	380, 440

**Table 2.3 Material properties randomly sampled to model the building stock.**

	Pre-code (all cases)	Low-code (all cases)
$R_{ck}$ [MPa]	35, 40, 45, 50 multiplied by $\gamma_c$	45, 50, 55 multiplied by $\gamma_c$
	<b>Smooth</b>	<b>Ribbed</b>
$f_{sk}$ [MPa]	$\mu = 356$ $\sigma = 67.8$	380 multiplied by $\gamma_s$
		<b>Ribbed</b>
		380, 440 multiplied by $\gamma_s$

**Table 2.4 Load cases randomly sampled as a function of the type of structures and the dimensions of the members.  $G_R$  is the roof weight,  $G_{LB}$  the lateral beam weight,  $G_B$  the beam self-weight,  $Q_1$  and  $Q_2$  the accidental and snow weight, respectively.**

Load Type		Type 1	Type 2
$G_R$ [kN/m <sup>2</sup> ]	$L_{intercol} < 20$ m	2.4	2.9
	$L_{intercol} > 20$ m		1.6
$G_{LB}$ [kN/m]		2.4	
$G_B$ [kN/m]	$L_{beam} < 16$ m	3.6	4
	$16 < L_{beam} < 22$ m	5.2	6
	$22 < L_{beam} < 24$ m	6.85	7.5
	$24 < L_{beam} < 28$ m	7.5	8
	$L_{beam} > 28$ m	8.55	9.5
$Q_1$ [kN/m <sup>2</sup> ]	normal distribution	$\mu = 2$ ; $\sigma = 0.4$ ; min = 0.8; max = 3.2	
$Q_2$ [kN/m <sup>2</sup> ]	normal distribution	$\mu = 2$ ; $\sigma = 0.4$ ; min = 0.8; max = 3.2	

Several probabilistic distributions (normal, lognormal, gamma) were considered for the characterisation of the geometric properties of precast structures. The maximum likelihood approach was adopted to select the probabilistic model that provided the best fit and the chi-square test was employed to evaluate the goodness-of-fit for a set of significance levels (1%, 5% and 10%), as described in Bal et al. [13]. For the cases for which the probability distributions showed a poor fit with the field data, a decision was made to use expert opinion to determine an adequate probabilistic model. All the parameters are described in Table 2.5, noting that minimum and maximum truncating values were defined by expert opinion, with a view to avoid unrealistic parameters.

**Table 2.5 Geometric dimensions randomly sampled for the generation of the building stock.  $\theta$  and  $\sigma$  are the median and dispersion, describing beam length ( $L_{\text{beam}}$ ), distance between portals ( $L_{\text{intercol}}$ ) and column height ( $H_{\text{col}}$ ).**

Structural Configuration		Distribution	$\theta$	$\sigma$	min	max	$\chi^2$ test	Source
Type 1	$L_{\text{beam}}$ [m]	Lognormal	14.9	0.3	8	30	10%	Tuscany database
	$L_{\text{intercol}}$ [m]	Lognormal	9	1	8	10	not passed	expert opinion
	$H_{\text{col}}$ [m]	Lognormal	6.5	0.25	4	12	not passed	Tuscany database
Type 2	$L_{\text{beam}}$ [m]	Normal	8.7	2.1	8	10	not passed	Tuscany database
	$L_{\text{intercol}}$ [m]	Normal	16.5	3.7	10	25	not passed	Tuscany database
	$H_{\text{col}}$ [m]	Normal	6.5	1.3	4	11	10%	Tuscany database

## 2.2 Design, numerical modelling and damage analyses

### 2.2.1 Design

The structures were designed in compliance with the pre-code and low-code classification, as previously noted. The DM 3-03-1975 [10] is the main reference for the pre-code typologies, and the DM 16-01-1996 [11] for the low-code design. In both cases the allowable tension method was employed, which consists in the comparison of the maximum values of stresses in the concrete and steel bars with those of the allowable ones. According to this design philosophy, the dimensions of a given member and the amount of steel reinforcement should increase until the stresses are lower than the limits of the materials. The seismic action is applied as static horizontal loads, corresponding to a fraction of the total weight of the building. This percentage is very low for the pre-code design (2%), whilst in the low-code it is a function of the seismic region where the structure is located (4%, 7% and 10% for seismic zones III, II and I, respectively). Moreover, in the low-code designed structures, second order (P-Delta) effects are taken into account, as well as the shear demand. These differences between the pre-code and low-code design are summarised in Table 2.6, while the full design methodology is presented in Casotto [14].

**Table 2.6 Summary of the pre-code and low-code design methods and requirements**

	Pre-code	Low-code
Seismic Action	Static Analysis	Static Analysis
	Horizontal force 2% of the total weight	Horizontal force for three classes S=6, 9, 12 P-Delta effects considered
Design Method	Admissible tension	Admissible tension
	Flexure and Compression for small eccentricity	Flexure and Compression for big eccentricity (computation of the neutral axis position)
	Standard shear reinforcement	Design of the shear reinforcement Verification of the displacements
Connections	Friction connection	Connections with standard steel elements

The type of connection considered in this study consists of a simple corbel supporting the roof beams. Further details about the design of the connections can be found in EOTA [15]. Connections relying on friction are allowed in the pre-code design, but not in the low-code, as stated in the DM 03-12-1987 [16]

regulations. Thus, in pre-code buildings the capacity of the connections was calculated simply as the friction resistance. The friction coefficient depends on the type of interface that supports the beam (concrete, rubber pads or steel plates). The definition of this parameter is a controversial matter, as in the literature it is found to vary between 0.6 and 0.9, whilst in some experimental campaigns lower values between 0.1 and 0.5 have been observed (Magliulo et al., [17]). Due to this uncertainty, a decision was made to adopt two fixed values of 0.2 and 0.3, the former close to the lower bound and the latter the mean of the range found in Magliulo et al. [17], and to estimate the effect of this parameter on the final fragility curves. The load variation due to the vertical acceleration was considered differently in the 2D and the 3D modelling frameworks, as will be explained in Section 2.2.3. For low-code structures, steel bolts or bars (so-called dowel connections) can be used to reinforce the connection. The resistance of the steel-concrete interaction is assumed to be the smallest between the shear resistance of the steel and that of the concrete.

### **2.2.2 Numerical modelling**

The randomly generated structures were modelled in both a 2D and 3D environment using the software OpenSEES [1], considering both the geometric and material nonlinearities. In the 2D framework the structure was represented by the external frame in the direction longitudinal to the main beams, because it is the frame with less axial load and thus more sensitive to connection failure. The concrete nonlinear behaviour was modelled using the proposal by Kent-Park and modified by Scott et al. [18], whilst the steel was simulated using the Menegotto and Pinto [19] model. The numerical model included material inelasticity in a distributed fashion, using force-based fibre finite elements for the columns, with a mesh of 220 fibres and 4 integration points.

Since the beams are pre-stressed precast members designed to remain elastic under the gravity loads, and the hinge connections do not allow the additional moments in the columns produced by the seismic action to be transmitted to the beams, for the sake of simplicity it was decided to represent them with elastic elements. To ensure that no moments are transmitted to the beams, link elements with no flexural stiffness were introduced at the top of the columns.

### **2.2.3 Damage analyses**

As mentioned before, two types of analysis were conducted: nonlinear static and nonlinear dynamic analysis. The former was undertaken to establish a set of limit states (levels of capacity) and the latter to simulate the seismic event and capture how the building responds to different levels of ground motion intensity in terms of internal forces and displacements (which are then compared with the aforementioned limit states). The analyses were repeated for the various typologies of precast industrial buildings, for the three levels of design lateral load (4%, 7% and 10% of the total weight) in the low-code design case, and for one level of design lateral load in the pre-code design case (2% of the total weight).

The overall process is summarised in Figure 2.2: the top images represent the pushover analysis of a single 2D frame, with the definition of the two limit states; the middle images present a single frame being tested against the suite of accelerograms through dynamic analysis, and the resulting maximum response overlapped with the pushover curves previously computed. The bottom images represent the repetition of the previous two steps for all the frames that constitute the randomly generated building stock.

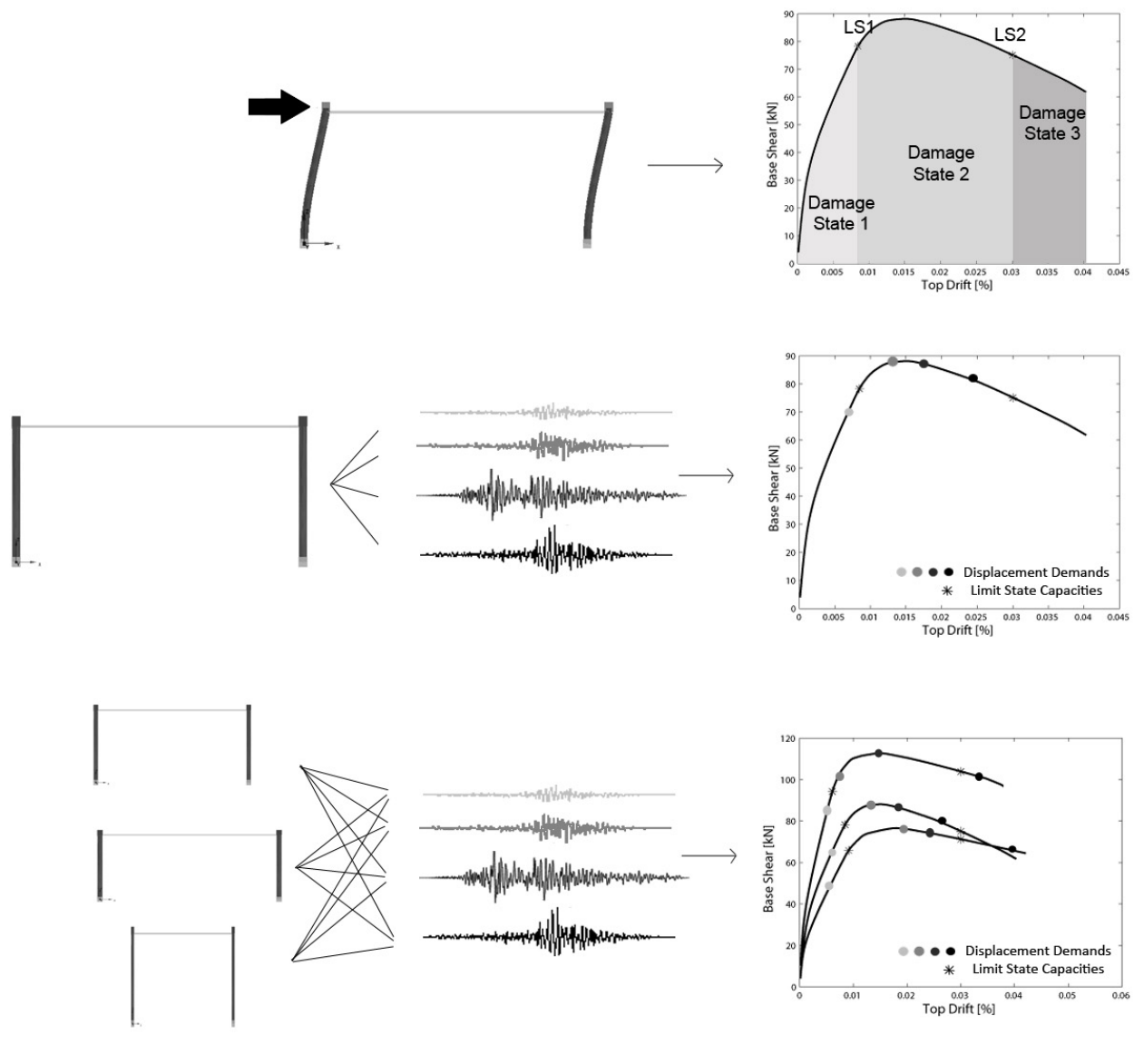


**Figure 2.2 Scheme of the analysis process, pushover analysis of a single building generating a pushover curve with limit states (top), dynamic analysis of a single building for multiple records (middle), dynamic analysis of the building stock for multiple records (bottom)**

### ***Pushover analysis and damage states definition***

A pushover curve was computed to estimate a set of limit state global drifts. There are many criteria that can be employed for the limit state definition according to the level of complexity of the models and of the analyses. Crowley et al. [20] considered damage limit states based on the strain levels in the concrete and steel, whilst other authors (e.g. Erberik [21]; Akkar et al. [22]) defined these thresholds using inter-storey drifts. Three damage states are applicable in this specific case: none/slight damage, moderate/extensive damage and collapse.

The member flexural strength, which characterises the first limit state (LS1), is attained when the reinforcement steel in the columns first yields. The ultimate strain limits of concrete  $\epsilon_c=0.005$  and steel  $\epsilon_s=0.015$  proposed by Crowley et al. [20] cannot be used to characterize the collapse limit state in this study, as they lead to excessive levels of top displacement. Furthermore, inter-storey drifts frequently suggested in the literature for damage criteria of RC structures are also inadequate, as traditional RC structures with

monolithic connections feature a very different response with respect to RC precast buildings with hinged beam-column joints. The main reason for this difference is the combination of slenderness and low transverse reinforcement ratio in the latter. In Deyanova et al. [23] different methodologies for defining the ultimate rotation of precast columns typical of the Italian constructions have been compared. These methods include the so-called “DDBD” method that follows the recommendations for yielding curvature, ultimate curvature and plastic hinge length by Priestley et al. [24]. Another approach was based on Cumbia, a moment-curvature software developed by the same authors, which calculates the displacement at expected buckling. A fibre-element based approach was also adopted and section analysis with the finite element software SeismoStruct [5] was performed. The ultimate drift of the columns was also evaluated following the approach by Haselton [25]; Fischinger et al. [26] found that this method best matched the experimental results amongst all those they investigated. The Haselton approach, however, yields unrealistic results for the Italian precast columns due to the very low transverse reinforcement ratio ( $\rho_{sh}=0.04\%$ ) compared to that of the structure tested by Fischinger et al. [26], where  $\rho_{sh}=0.86\%$ . As far as the ultimate displacement was concerned, all the methods used by Deyanova et al. [23] gave a wide range of results. It is clear that more investigation is needed in this field and in the meantime the flexural collapse limit state (LS2) has been set to 3% inter-storey drift, as experimentally verified by Brunesi et al. [27].

Failure due to shear was not considered in the present study because it has not been observed in any of the precast industrial structures investigated after Emilia-Romagna events (Deyanova et al. [23]). The reasons why flexural collapse was predominant include the large column sections, designed for instability and buckling, and the slenderness of the columns, due to the large inter-storey height.

The collapse limit state is related also with the loss of support of the beam. The connection collapse is evaluated differently in the 2D and 3D framework, and with two different approaches in the 2D framework. The two approaches in the 2D environment differ in the way the friction capacity is calculated and in the consideration of sliding of the beam on the column support. In the first approach, connection collapse is identified when the shear demand in at least one column exceeds the connection capacity; the capacity of the connection is computed assuming a constant force, proportional to 40% of the axial load (as applied in Bolognini et al. [4]). In the second method this capacity is dependent on the vertical component of the ground motion records and collapse is identified only when the sliding displacement of the beam exceeds its support length and unseating occurs. Sliding has been accounted for with Newmark sliding block analysis (Figure 2.3), adopted from Kramer [28]: the sliding displacement is computed as the double integration of the acceleration at the connection node exceeding the yield acceleration benchmark (shaded grey area shown in Figure 2.3), which is the acceleration corresponding to the connection resistance force.

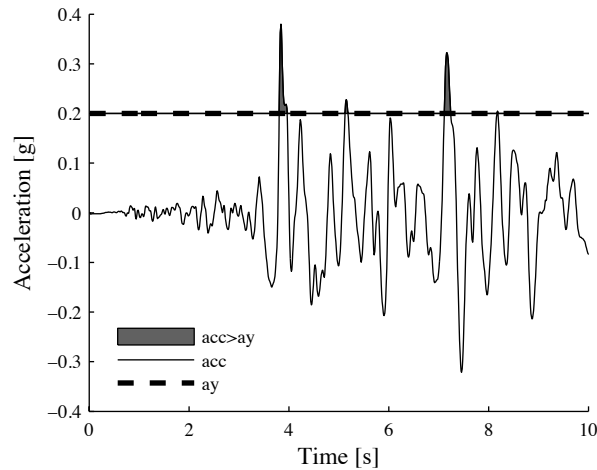


**Figure 2.3 Newmark sliding block analysis for the evaluation of sliding displacement**

The yield acceleration benchmark  $a_y$  is computed as in the following equation:

$$a_y = \frac{V_{cnn}}{m}$$

where  $m$  is the inertial mass at the connection location and  $V_{cnn}$  is the shear capacity of the connection, a function of the friction coefficient and the axial load  $N$ . If  $N$  is not considered constant but varying with the vertical acceleration, the yield acceleration  $a_y$  will not be a horizontal line as in the figure above, but it will also vary in time. The support length is computed as half of the corbel length, to consider the worst case scenario where the columns oscillate out of phase.

Figure 2.4 shows the limit states evaluated on the pushover curve including connection collapse limit state computed with the constant connection resistance. For this particular case, collapse due to connection failure is reached before the other two limit states.

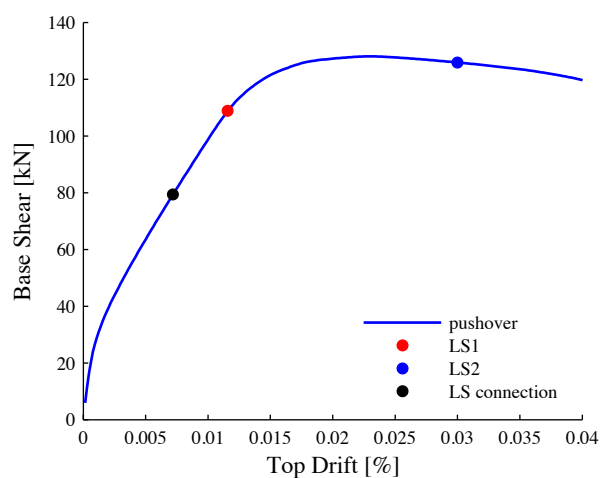


**Figure 2.4 Pushover curve and limit states for a structure representative of T1-PC-2 typology**

The 3D modelling framework introduces an additional source of complexity in the pushover analysis regarding the direction in which the pushover should be performed to define the limit states. Given the

simplicity of this type of structure (i.e. single-storey buildings) a 3D displacement-based pushover was applied, wherein the increments in each direction were proportional to the stiffness in the corresponding direction, in order to approximate the progressive deformation of the structure subjected to a horizontal seismic force in the 3D space. Two other pushover analyses were performed loading the structure in the two directions separately, checking whether the x and y components of the limit states evaluated on the 3D bi-directional pushover curve exceed the limit states obtained when loading only in one direction. In this case, the damage induced by a mainly x- or y-oriented seismic excitation could be underestimated, and for this reason, after the dynamic analysis, the uni-directional limit states are used for the comparison with the x and y maximum displacements, whilst the limit states derived with the bi-directional pushover curve are compared with the modulus of the displacement vector. The structure is finally allocated to the maximum damage state resulting from the three aforementioned comparisons. The limit states were defined on each pushover curve, using the same criteria described for the 2D framework. Connection failure, which leads to sudden collapse of the structure, was considered to occur when the sliding displacement is exceeded in at least one direction, considering the two directions separately. The test in each direction is carried out in the same way as in the 2D approach with vertical acceleration.

### ***Dynamic analysis and seismic input***

To the previously described structural model the following additions were made for the dynamic analyses: the masses were lumped at the joints and a tangent stiffness proportional damping model was used with a damping ratio of 2%. Two types of dynamic analyses were performed on the 2D frames; considering only one horizontal input or applying both the horizontal and the vertical accelerations, thus allowing the calculation of the connection capacity as a function of the vertical excitation. The maximum response of the structure, expressed in terms of maximum top drift, was compared with the drift limits defined with the pushover analysis to allocate each frame into a damage state. In the 3D environment the structures were subjected to accelerograms in the three directions and the maximum top displacements in x and y and the modulus of the displacement vector were compared with the three sets of limit states derived with the uni-directional and the bi-directional pushover curves respectively, as previously described. The contributions in terms of damage state per level of ground motion intensity, obtained from all the samples subjected to all the records, were summed up and normalised with respect to the total number of buildings to compute the Damage Probability Matrix (DPM). This matrix contains the percentage of frames in each damage state for a set of intensity measure levels representing each ground motion record.

The use of real accelerograms for defining the input to dynamic analyses was adopted (as opposed to employing synthetic or artificial records, in which the scaling process might lead to unrealistic properties in the ground motion records, such as frequency content and/or duration). Stewart et al. [29] and Bommer and Acevedo [30] considered magnitude (M) and distance (R) as important parameters for the earthquake record selection, complemented by the soil profile (S) at the site of interest, leading to (M, R, S) record sets. The region of interest is Northern Italy, with particular focus on the region of Emilia-Romagna, where the ranges of these parameters contributing to the 475 years return period hazard for  $S_a(T=1.5 \text{ sec})$  are Mw from 4 to 6.5 and R from 0 to 20 km, whilst those contributing to the 2475 years return period are Mw from 4.5 to 6.5 and R from 0 to 30 km (Iervolino et al. [31]). The soil in this area is classified by Borzi and Di Capua [32] as soft, according to the EC8 soil classes, or as category C and D, following the Italian code classification (NTC2008 [33]). Seventy accelerograms in the three directions (leading to 210 records) were extracted from the PEER database [6]. A low scaling factor of approximately 1.5 was applied to 13 of the ground motion records in order to simulate stronger intensity measure levels, which is an acceptable factor according to Watson-Lamprey and Abrahamson [34]. Moreover, records with directivity or pulse effects were avoided. The histograms of PGA and  $S_a(T=1.5 \text{ sec})$  are presented in Figure 2.5.

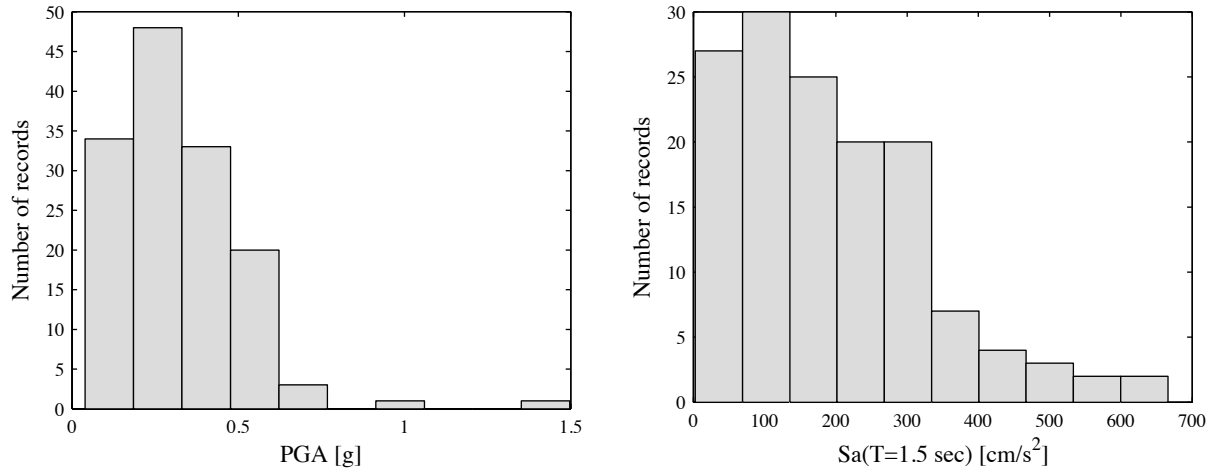


**Figure 2.5 Histograms of PGA (left) and  $S_a(T=1.5 \text{ sec})$  (right) of the selected horizontal ground motion records.**

### 2.3 Fragility curve derivation

The results from the nonlinear dynamic analyses were assembled in the Damage Probability Matrix, which contained the fractions of sampled structures in each damage state, for a set of increasing intensity measure levels. Then, the cumulative fraction of structures in each damage state was estimated, by summing the percentages of frames belonging to all the subsequent damage states. A lognormal cumulative distribution function, expressing the probability of exceeding each damage state in a continuous fashion, was then fit to these results. The regression analysis was carried out using the maximum likelihood method.

In the 2D approach, that hypothesizes a 40% axial load reduction to account for vertical acceleration, a simplified methodology was employed to include the Probability of Exceedance (PoE) of connection failure. This probability was computed separately and then added to the PoE of flexural failure to obtain the total PoE of the ultimate limit state. In fact, the discrete probabilities for increasing intensity of the ground motion were very scattered and the dispersion was high when trying to fit them with a unique continuous function. The dispersion decreased considerably considering the two conditional probabilities separately, because they are able to describe the two trends visible in the collapse fragility curves (Figure 2.6): a first trend when the demand is not enough to attain flexural capacity and collapse is due only to connection failure, and a second trend when flexural failure starts contributing to collapse, while connection failure is limited by the maximum percentage of frames featuring the connection collapse mechanism. The total PoE of collapse is the sum of the two conditional probabilities: the probability of attaining connection collapse,  $P(C_{\text{Connection}})$ , conditional on the probability of presenting connection failure mechanism,  $P(\text{Connection mechanism})$ , and the probability of reaching flexural failure,  $P(C_{\text{Flexure}})$ , conditional on the probability of having flexural failure mechanism,  $(1-P(\text{Connection mechanism}))$ . The relation to estimate the total probability of exceeding collapse (PoE<sub>C</sub>) is thus expressed in the following equation:

$$\text{PoE}_C = P(C_{\text{Connection}})P(\text{Connection mechanism}) + P(C_{\text{Flexure}})(1-P(\text{Connection mechanism}))$$

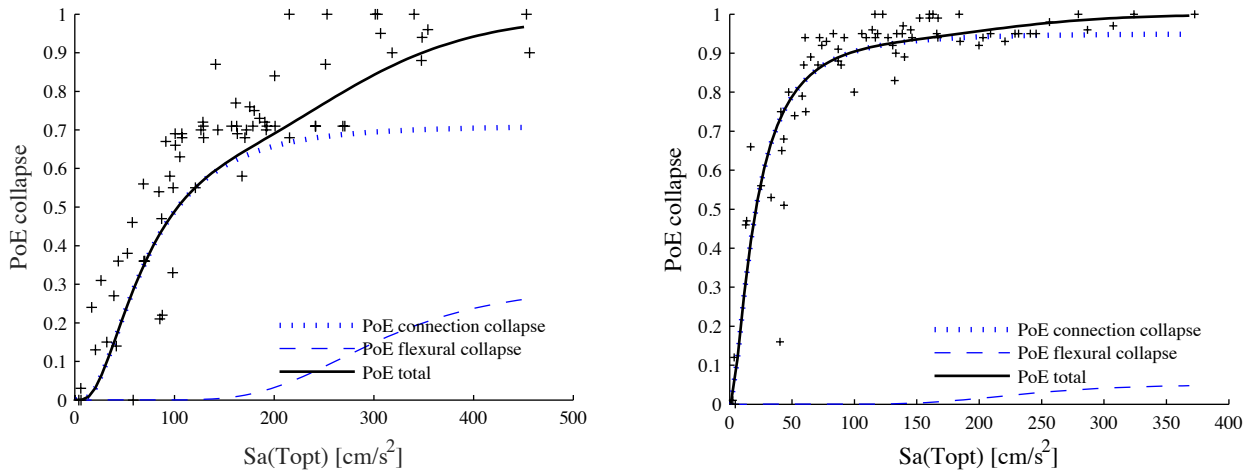


**Figure 2.6 Total probability of exceedance for the collapse limit state as the sum of the two conditional probabilities of flexural collapse and connection collapse, T1-PC-2 with 0.2 (left) and 0.3 (right) friction coefficient.**

The results of this simplified method are analysed in Figure 2.7, comparing the collapse fragility curves that comprise both failure mechanisms (flexure and collapse) with those that consider only flexural collapse, and with the yielding fragility curve. The comparison shows that connection collapse plays an important role in the total collapse curve, but also that for the typology in the plots it is more likely to occur than yielding, as similarly shown in Figure 2.4. This outcome reveals that the criteria used to assess connection failure (reducing by 40% the axial load and neglecting the unseating displacement of the beam) were too conservative, leading to unreliable results. The method was therefore discarded in favour of the other two approaches, where the beam-column joint collapse is assessed in a more accurate way. Moreover in the second approach implemented within the 2D framework and in the one applied within the 3D framework, a unique regression analysis was performed with the data comprising both flexural and connection failure, without the need to compute the PoE of connection and flexural collapse separately.

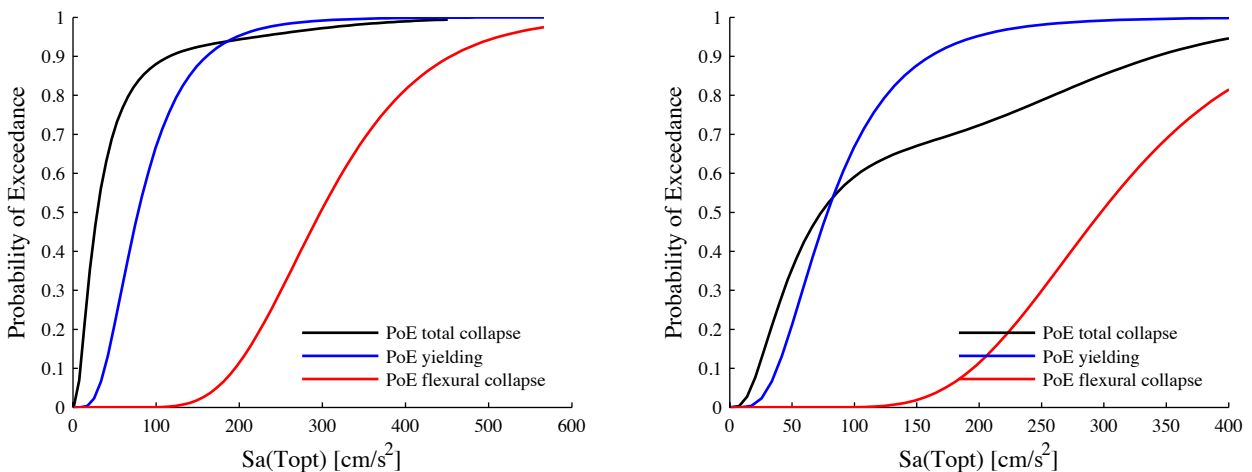


**Figure 2.7 Comparison between the total collapse fragility curve and the flexural collapse and yielding fragility curves, T1-PC-2 with 0.2 (left) and 0.3 (right) friction coefficient.**

A key point in the derivation of fragility curves is the selection of the intensity measure (IM) that adequately correlates with damage. Various intensity measures were considered and compared, using the  $R^2$  coefficient to quantify the correlation between the intensity levels and the cumulative percentage of frames for each

limit state. The peak ground acceleration (PGA) is a very common measure in vulnerability studies, as Crowley et al. [35] showed when collecting more than four hundred fragility curves. This parameter is also easily extracted from ground motion records; however, for structures with long fundamental periods of vibration, this IM leads to very large dispersion in the results (see Figure 2.8).

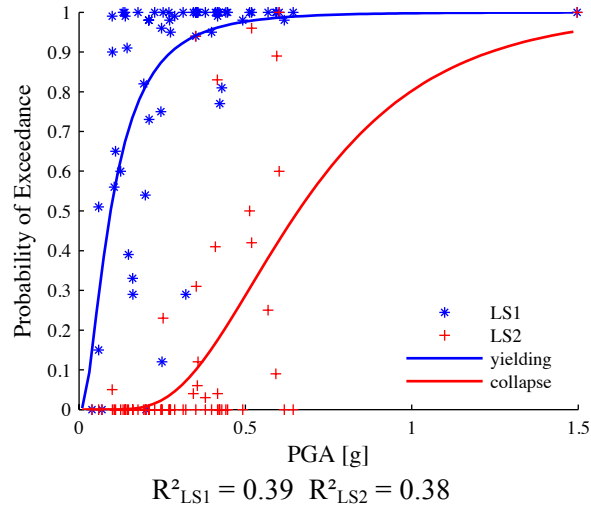


**Figure 2.8 Fragility curves using PGA and correlation coefficients  $R^2$  for typology T1-PC-2**

The employment of a spectral quantity, such as spectral acceleration ( $S_a$ ), introduces the problem of selecting the period for which the spectral ordinate is computed. In fact, the selected period is of great importance for the reduction of the uncertainty in each limit state curve. The elastic period is a common choice, but it is not very representative of the dynamic properties of a structure, as even for low intensities the cracking of concrete elongates the period of vibration significantly. Silva et al. [36] investigated the influence of the period of vibration on the variability of the fragility curves, by computing the coefficient  $R^2$  for a set of elastic periods. The same correlation analysis was carried out for RC precast industrial buildings, as shown in Figure 2.9. The mean  $R^2$  curve (the mean between the first limit state and the second limit state  $R^2$  curves) is also presented and the optimal period (the periods corresponding to the maximum correlation for each limit state and for the mean curves) is indicated with a vertical line. The spectral acceleration at the mean optimal period of vibration  $S_a(T_{opt})$  increases the performance of the second limit state curve (which provides information about the damage state that has a larger influence on the losses) without substantially compromising the first limit state correlation.

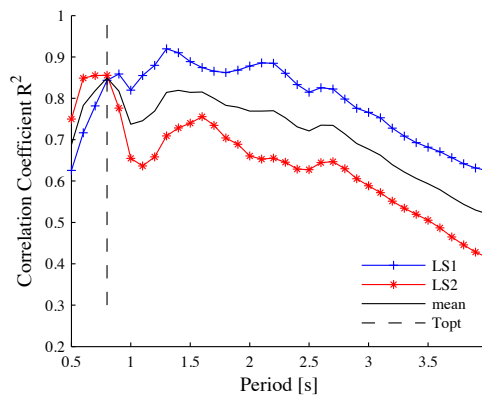


**Figure 2.9 Correlation coefficient as a function of the period of vibration of  $S_a$ , for T1-PC-2 typology.**

The main drawback of using  $S_a$  at the optimal period, as discussed by Vamvatsikos and Cornell [37], is that it does not correspond to the period of vibration of the structure at a certain condition of damage and it would be difficult to select *a priori*. The only way to estimate it robustly would be through a correlation analysis similar to that previously described, carried out for each typology, since a slight change in period could penalise the dispersion considerably. As an alternative, the power-law form with three spectral values ( $IM_{pw}$ ) proposed by Vamvatsikos and Cornell [37] was tested on the precast structures. The  $IM_{pw}$  combines the  $S_a$  for different spectral periods selected *a priori* in the following way:

$$IM_{pw} = S_a(\tau_a) \left[ \frac{S_a(\tau_b)}{S_a(\tau_a)} \right]^\beta \left[ \frac{S_a(\tau_c)}{S_a(\tau_a)} \right]^\gamma$$

where  $\tau_a, \tau_b$  and  $\tau_c$  are  $T_1, 150\%$  of  $T_1$  and  $200\%$  of  $T_1$  respectively, and  $T_1$  stands for the first period of vibration. In the original proposal, the period of the first vibration mode ( $T_1$ ), was computed for the elastic period. However, during the various analyses within this study, it was observed that the yielding period provided a considerably better performance, and so it was used instead of the elastic period. The comparison between the IMs explored so far, shown in Figure 2.8 and Figure 2.10, reveals the good performance of spectral quantities with respect to PGA and the similar effect of  $S_a(T_{opt})$  and  $IM_{pw}$  on the dispersion reduction.

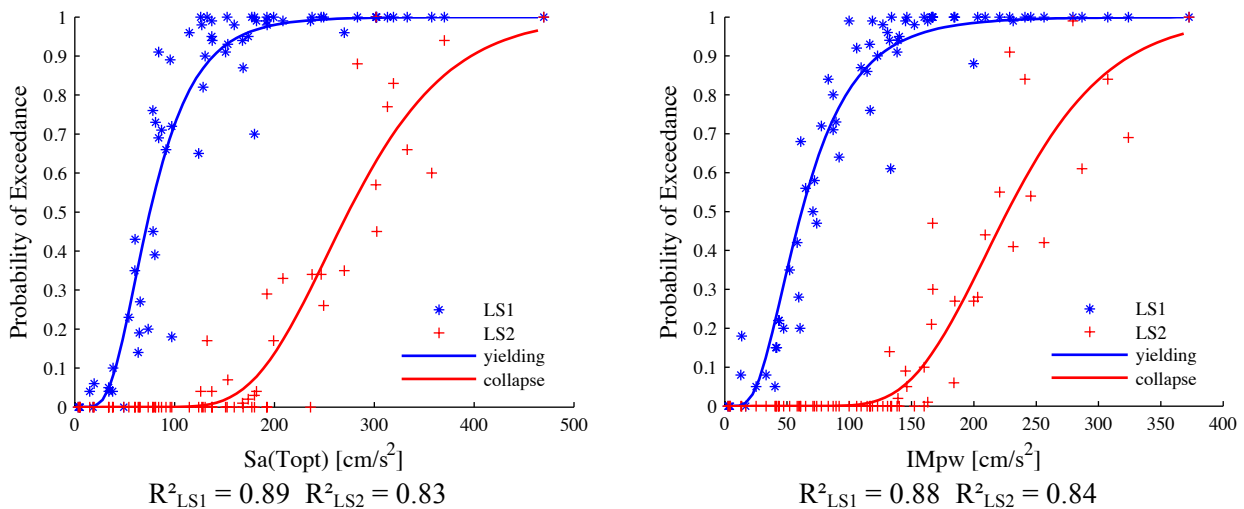


**Figure 2.10 Fragility curves for T1-PC-2 and corresponding correlation coefficients  $R^2$  as a function of IM used:  $S_a(T_{opt})$  (left),  $IM_{pw}$  (right). Only flexural collapse fragility curves are compared.**

Other IMs were tested, such as Arias Intensity and Cumulative Absolute Velocity, which considers the total energy stored during the seismic event, but showed to provide a weaker performance than the aforementioned IMs. Moreover, since the purpose of this study is to provide a set of fragility functions for earthquake loss assessment,  $S_a(T_{opt})$  was preferred to  $IM_{pw}$ . In fact even if  $IM_{pw}$  could be easily estimated from the  $S_a$  values directly provided by most of the ground motion prediction equations available in common seismic risk software, the cross correlation between the spectral ordinates combined in this parameter (see e.g. Baker and Jayaram [38]) would need to be estimated, which would significantly complicate the loss assessment methodology.

For what concerns the 3D analyses, the structures evaluated herein were no longer dominated by a single vibration mode, but usually by two modes with similar modal contribution in each direction, as well as a

similar elastic period. It was decided to use the geometric mean between the two horizontal components and the period that provides the better correlation coefficient according to the correlation analysis previously described. The geometric mean is now the most widely used horizontal-component definition in ground motion prediction equations (Beyer and Bommer, [39]), which is essential for the application of the derived fragility curves in loss models. The geometric mean is defined as:

$$S_{a,G\text{Mxy}}(T_{\text{opt}}) = \sqrt{S_{a,x}(T_{\text{opt}}) S_{a,y}(T_{\text{opt}})}$$

### 3 PROPOSED FRAGILITY FUNCTIONS

#### 3.1 Fragility curves

The final fragility curves derived within the 2D and 3D framework that include vertical acceleration in the dynamic analyses and unseating of the beam are presented in this section. Results for the hypothesis of 40% axial load reduction to account for vertical acceleration were discarded, as explained in Section 2.3. An example of the fragility functions obtained within the 2D and 3D environments is presented in Figure 3.1, while the parameters for yielding and collapse fragility curves are reported in Table 3.1. It should be noted that a direct comparison between the fragility curves derived with these two approaches is not reliable; despite the same intensity measure type being displayed on the x axis, they correspond to different optimal periods ( $T_{\text{opt}}$ ) and the geometric mean between the spectral acceleration of the two horizontal components is used in the 3D analyses, whilst the spectral acceleration from a single direction is used in the 2D analyses. These functions would need to be applied within a complete loss assessment exercise in order to fully appreciate the difference between them.

**Table 3.1 Results from the 2D and 3D approaches considering the vertical acceleration. Median ( $\theta$ ) and logarithmic standard deviation ( $\sigma$ ), and coefficient of correlation ( $R^2$ ) of each fragility function using friction coefficient of 0.2 and an intensity measure of  $S_a(T_{\text{opt}})$  in  $\text{cm/s}^2$ .**

Typology	2D							3D						
	$T_{\text{opt}}$	LS1			LS2			$T_{\text{opt}}$	LS1			LS2		
		$\theta$	$\sigma$	$R_{\text{LS1}}^2$	$\theta$	$\sigma$	$R_{\text{LS2}}^2$		$\theta$	$\sigma$	$R_{\text{LS1}}^2$	$\theta$	$\sigma$	$R_{\text{LS2}}^2$
T1-PC-2	0.8	216	0.59	0.84	376	0.55	0.86	2.3	44	0.56	0.94	128	0.26	0.93
T1-LC-4	1.6	96	0.48	0.88	306	0.42	0.83	2.3	44	0.53	0.91	133	0.39	0.88
T1-LC-7	0.8	276	0.46	0.88	609	0.56	0.81	1.4	112	0.41	0.93	277	0.55	0.66
T1-LC-10	0.8	302	0.38	0.93	392	0.53	0.87	0.7	258	0.49	0.84	403	0.52	0.90
T2-PC-2	1.7	79	0.51	0.89	166	0.54	0.74	2.2	38	0.52	0.91	125	0.23	0.91
T2-LC-4	1.7	80	0.47	0.90	255	0.39	0.86	2.3	43	0.46	0.94	121	0.34	0.88
T2-LC-7	0.8	240	0.46	0.88	554	0.45	0.80	1.4	99	0.37	0.96	235	0.47	0.64
T2-LC-10	0.8	270	0.41	0.93	379	0.51	0.86	0.7	221	0.48	0.78	422	0.46	0.78

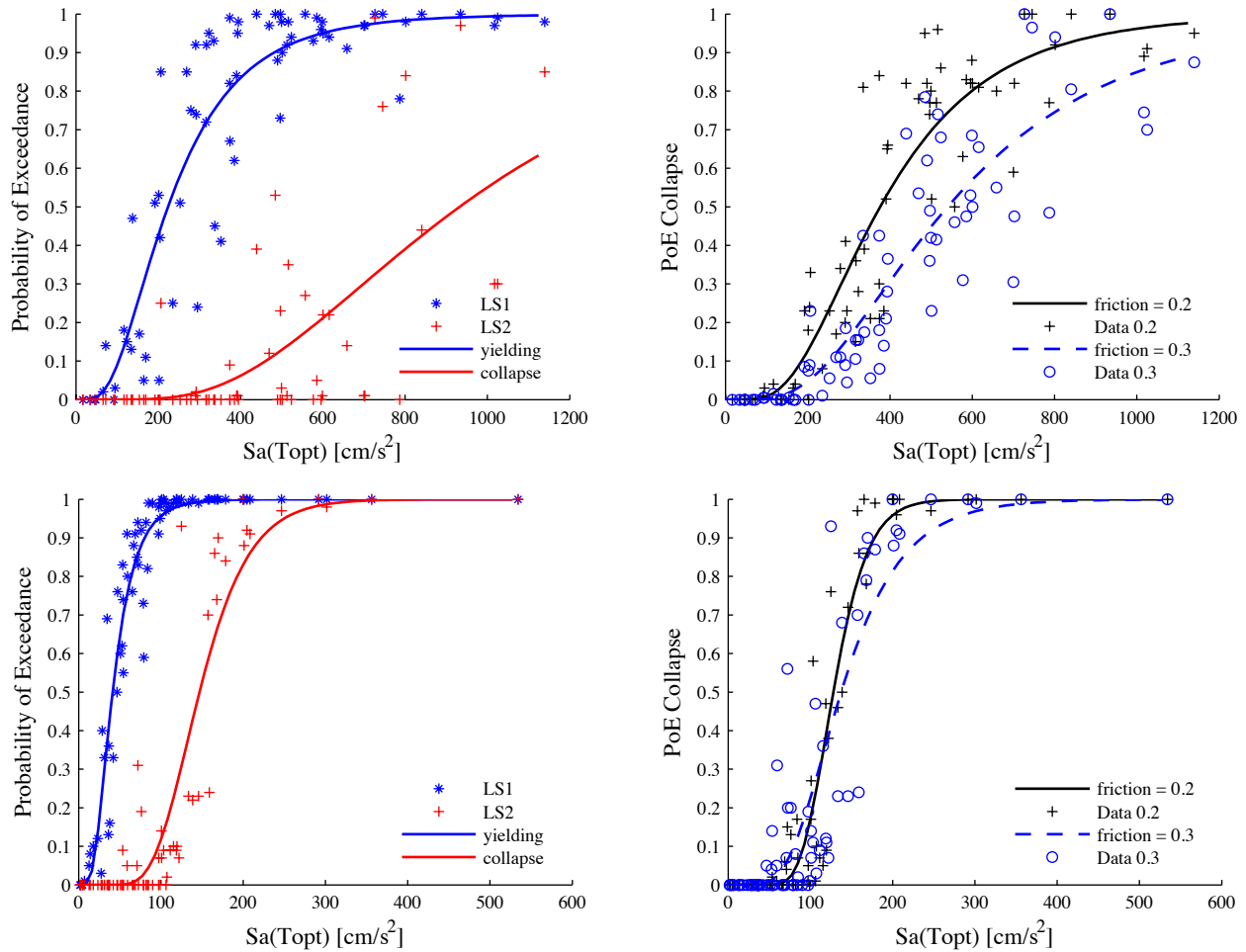


**Figure 3.1** Probability of exceedance derived in a 2D framework (top) and in a 3D framework (bottom) considering the vertical acceleration component. T1-PC-2 yielding and flexural collapse fragility curves (left), flexural and connection collapse curves (right) for the two friction coefficients.

### 3.2 Discussion

It is clear from the comparison between collapse fragility curves with and without consideration of connection failure in Figure 3.1 that connection collapse is an important issue that cannot be neglected and has to be addressed carefully. Connection failure occurs only if the shear demand on the top of the column exceeds the shear capacity of the connection and the beam unseats from the column support. This is the case only if the column is able to carry and transmit a force equal to or larger than the connection resistance, according to the hierarchy of the capacities. This is the reason why connection collapse is much more frequent in structures with friction-based connections or in the frames with stiff columns designed for higher lateral forces. Moreover, the chosen method used to evaluate this particular failure mechanism can influence the results considerably.

In the first methodology, connection failure is estimated based on constant column capacity and constant connection capacity (proportional to the initial axial load reduced by 40%). The base shear, when the connection capacity is reached in at least one column, is found on the pushover curve and defined as the connection collapse limit state, represented in Figure 3.2 by a horizontal dotted line. Connection collapse mechanism is thus evaluated at the beginning of the pushover analysis as the base shear at which the pushover curve of the structure exceeds the connection collapse limit state (Figure 3.2 left). This method

does not consider the possibility that the column capacity could be very close to the connection capacity (Figure 3.2 right) and it could easily exceed it during an acceleration time-history, where both the capacities vary with the vertical acceleration. Similarly it does not consider that the connection capacity could be exceeded, but the beam could still not be unseated because of its limited sliding displacement. The connection collapse is thus almost independent of the seismic input, because the connection limit state is set a-priori with the pushover analysis and it nearly corresponds to the yielding limit state, easily attained by weak ground motions. This is why for those typologies significantly affected by connection failure the collapse fragility curve can be even more fragile than the yielding curve (see Figure 2.7). The difference in the response between presenting and not presenting connection collapse limit state is drastic (in the former case failure can occur even before the building reaches yielding), and therefore it generates a large scatter in the fragility curves. Furthermore, when following this methodology the number of frames with connection collapse mechanism is very sensitive to the friction coefficient. Given the large uncertainty in the friction coefficient definition, the consequent impact on the fragility curves, and especially the excessive fragility of collapse curves with respect to yielding curves, as discussed previously, this method was considered unreliable and it was thus discarded.

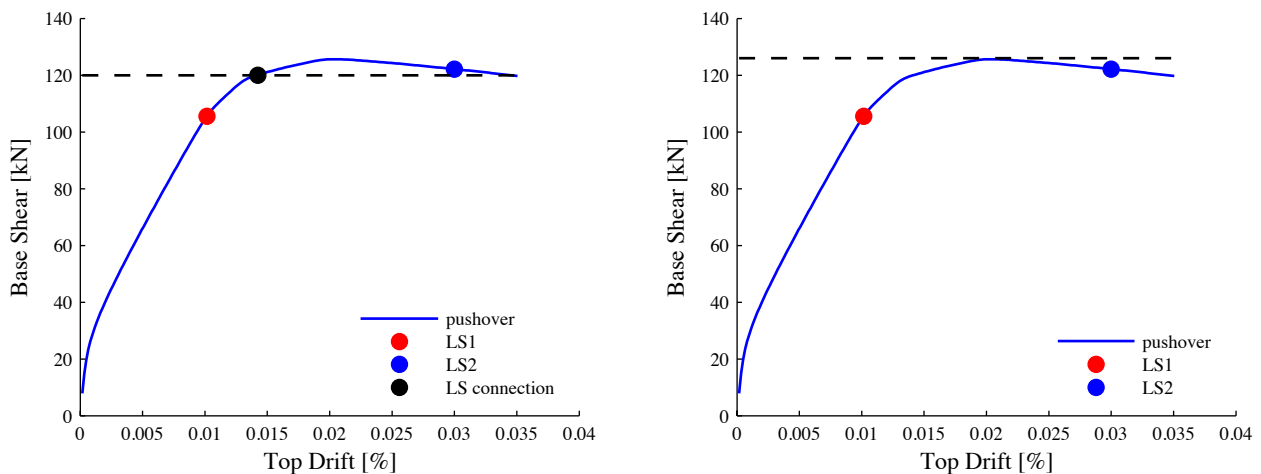


**Figure 3.2 Connection collapse limit state definition: 2D with constant connection resistance method. Frame presenting connection collapse limit state (left) and frame not presenting connection collapse limit state (right).**

In the methods where the connection capacity is affected by the vertical component of the acceleration and the unseating of the beam is considered, the aforementioned issue is overcome by assessing connection collapse when the shear demand time-history crosses the connection resistance time history and the sliding displacement of the beam exceeds the support length (Figure 3.3). In this case, the friction coefficient seems to have a smaller impact, because the connection collapse mechanism is now sensitive to the vertical component of the ground motion record, and the transition between collapse fragility curves calculated using different levels of friction coefficient is smoother, as shown previously in Figure 3.1.

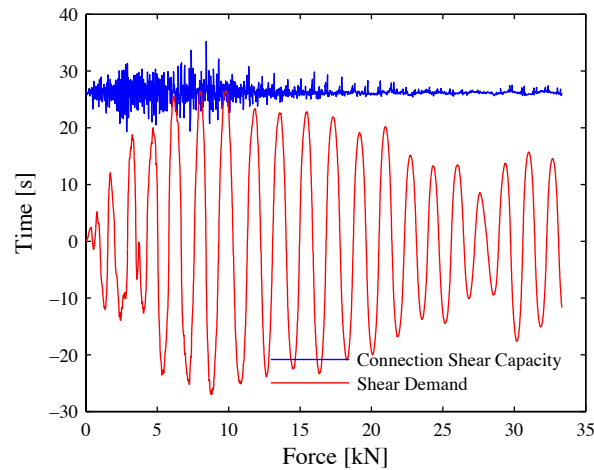


**Figure 3.3 Connection collapse limit state definition: 2D environment with connection capacity based on the vertical acceleration component.**

### 3.3 Comparison with field data

In order to have an initial consistency check on the reliability of the results obtained herein, a first comparison with data from a field survey of 1133 precast industrial buildings after the 2012 Emilia Romagna earthquakes has been performed. Empirical fragility curves were derived by Minghini et al. [40] in terms of the largest between the two horizontal components of  $S_a$  at 1 second, for three damage states: no damage (D0), slight damage/moderate damage (D1+D2), severe damage/heavy damage/collapse (D3+D4+D5). In the study by Minghini et al. [40] the surveyed buildings are not classified according to the age of construction or the geometric typology, therefore a single fragility function is available for the comparison.

Given the features of the empirical curves the following modifications on the analytical method used were needed to harmonise the damage scales and the building typologies:

- Collapse limit state (LS2), defined herein as flexural or connection failure, was considered equivalent to the onset of D3+D4+D5 in Minghini et al. [40] (though it is recognised that DS5 would have been a better damage state for comparison purposes, had the results for this damage state been available).
- A single DPM was assembled summing up the number of buildings in each damage state resulting from the dynamic analysis run for the typologies considered appropriate for Emilia Romagna, the Italian region where the damaged data were taken from. Considering that the Emilia Romagna region was classified as seismic only in 2003, the pre-code typology (PC-2) and the low-code typology with the minimum design lateral load (LC-4) were thought to better represent the building population of the area. Both geometrical configurations were included with equal weight in the total DPM, given that the damage data do not contain this type of information.
- A regression analysis was run on the total DPM obtained, using as intensity measure the largest value between the two horizontal components of  $S_a$  at 1 second.

Figure 3.4 shows the resulting fragility function for a single typology using the 2D modelling environment, whose median is 0.56 g for LS2, while Figure 3.3 represents the discrete empirical fragility functions. It can be observed in Figure 3.5 that the value at 50% of the cumulative frequency of occurrence is 0.42 g; in the case of the highest damage state this value corresponds also to the median of the probability of exceedance. In order to evaluate this comparison it must be considered that the buildings damaged in the Emilia region were subjected to at least two strong earthquakes, and thus the final damage states observed in some structures might have been due to cumulative damage. Hence, the Minghini et al. [40] fragility functions might present lower median values than would be expected for these structures under a single event.

Furthermore, the DS3+DS4+DS5 damage state from Minghini et al. [40] includes structures that have not collapsed, and so again this data is expected to produce lower median values than would be expected for collapsed buildings alone. Hence, it is reassuring that the median fragility functions presented herein produce higher median values compared to the observed damage data, but further conclusions cannot be drawn given the large number of approximations in the comparison.

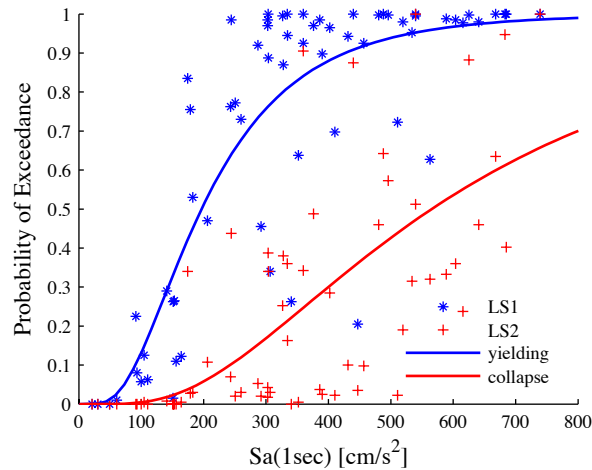


Figure 3.4 Analytical fragility function for a single typology using the 3D modelling environment.

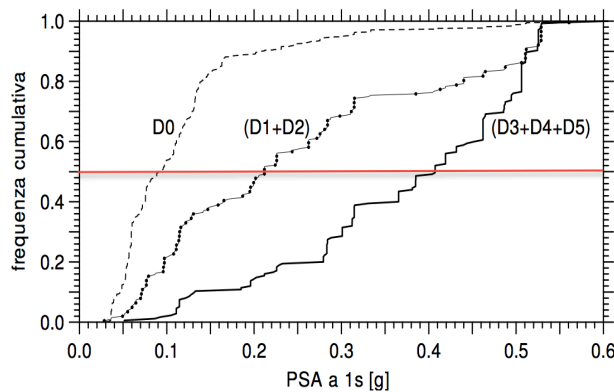


Figure 3.5 Empirical cumulative frequency of occurrence vs  $Sa(T=1sec)$  [Minghini et al. [40]].

## 4 CONCLUSIONS

The aim of this study was to develop a robust methodology to derive fragility curves for precast RC industrial buildings. A large portion of the RC industrial buildings were designed essentially for static horizontal loads and with simply supported beam-column joints, and could thus be particularly vulnerable to the dynamic input from earthquakes. In the current literature there seems to be limited experience in the fragility assessment of such structures, and for this reason it is important to investigate how inevitably necessary simplifications in structural modelling and fragility methodology, commonly applied to regular cast-in-place buildings, may or may not influence the fragility assessment of these precast buildings.

A set of fragility curves has thus been developed, considering the main characteristics of these structures: the weak beam-column connections, which is the principal cause of total collapse of the building due to loss of support of the beams, even for moderate earthquakes. The variability in the fragility curves with respect to

the simplifications in modelling and type of analysis was studied, through the application of a nonlinear dynamic procedure in three different manners: in a 2D environment where the frames were tested against horizontal accelerograms only in their main direction and the influence of the vertical acceleration was simulated by reducing the axial load by 40% (Bolognini et al. [4]); in a 2D environment considering the vertical input of the ground motion records; and finally in a 3D environment where all the three components of the earthquake records were considered. Connection failure was explicitly accounted as a collapse limit state.

The comparison between collapse fragility curves with and without consideration of connection failure demonstrated the importance of considering connection collapse mechanism and representing it robustly. In fact, the outcomes of the 2D analysis without vertical acceleration highlighted some drawbacks regarding the connection failure determination. This approximate method rendered the collapse fragility curves more sensitive to the friction coefficient used to compute the connection capacity rather than to the ground motion intensity. Given the large uncertainty in the definition of the friction coefficient and the drastic changes in the fragility curves corresponding to small variations of this parameter, this method was discarded. When applying a vertical acceleration in the dynamic analyses both in the 2D and 3D framework, the transition between different levels of friction coefficient was much smoother. In order to be conservative, the final fragility curves were computed using a friction coefficient of 0.2, but it is underlined that this parameter requires further research and calibration.

A direct comparison between the 2D and 3D approaches with vertical acceleration is not straightforward, due to the discrepancies in the IMs and structural aspects considered within each approach. However, the results from this study seem to indicate that a higher fragility is obtained when considering the three components of the earthquake record. The actual differences between the 2D and 3D approaches can only be appreciated through the employment of the respective fragility functions in a case-study risk assessment application, which will be carried out as a further development of this work.

A deeper understanding of the structural aspects involved in the fragility assessment of this specific type of structure has been reached herein. Particular attention has been paid to the connection collapse phenomenon, and the importance of the selection of the proper methodology to assess it accurately has been demonstrated. Finally, a preliminary comparison has been performed with damage data from field surveys of the 2012 Emilia Romagna earthquakes and a good agreement between the analytical and empirical functions was observed despite the inevitable approximations in the harmonisation of the empirical and analytical data.

It can be concluded that a sound set of fragility functions for Italian industrial precast buildings is now available for earthquake loss assessment, which could be employed for the development of seismic risk mitigation actions.

## **5 ACKNOWLEDGEMENTS**

The authors would like to thank the Seismic Risk Prevention Area of Tuscany Region, who kindly shared their database regarding the geometrical properties of the industrial structures. The authors are very grateful for the valuable contribution of Davide Bolognini, whose expert advice on Italian precast structures is most appreciatively acknowledged. The authors are also very grateful to Anže Babič, Manya Deyanova and Matjaž Dolšek for discussions and input on the seismic behaviour of RC precast industrial buildings which helped improve the collapse limit state modelling used herein. The authors would like to express their gratitude for the comments and the suggestions of the reviewers, that helped to improve significantly the quality of the paper. Finally, the authors would like to acknowledge the support provided by the European

Commission under FP7 through the financing of the STREST research programme, under the framework of which this work has been partially funded.

## 6 REFERENCES

- [1] Belleri, A., Brunesi, E., Nascimbene, R., Pagani, M., Riva, P. [2014] "Seismic performance of precast industrial facilities following major earthquakes in the Italian territory," *Journal of Performance of Constructed Facilities*, doi: 10.1061/(ASCE)CF.1943-5509.0000617
- [2] Calvi, G.M., Pinho, R., Magenes, G., Bommer, J.J., Restrepo-Vèlez, L.F., Crowley, H. [2006] "Development of seismic vulnerability assessment methodologies over the past 30 years," *ISET Journal of Earthquake Technology*, Vol. 43, No. 3, pp. 75-104.
- [3] Borzi, B., Pinho, R., Crowley, H. [2008] "Simplified pushover-based vulnerability analysis for large-scale assessment of RC building," *Engineering Structures*, Vol. 30, No. 3, pp. 804-820.
- [4] Bolognini, D., Borzi, B., Pinho, R. [2008] "Simplified Pushover-Based Vulnerability Analysis of Traditional Italian RC precast structures," *Proceedings of the 14th World Conference on Earthquake Engineering*, Beijing, China.
- [5] Senel, M.S., Kayhan, A.H. [2010] "Fragility based damage assessment in existing precast industrial buildings: A case study for Turkey," *Structural Engineering and Mechanics*, Vol. 34, No.1, pp. 39-60.
- [6] Ordinanza del Presidente del Consiglio dei Ministri n. 3274 del 20 marzo 2003 [2003] "Primi elementi in materia di criteri generali per la classificazione sismica del territorio nazionale e di normative tecniche per le costruzioni in zona sismica," (in Italian).
- [7] Calvi, G.M., Bolognini, D., Nascimbene, R., [2006] "Seismic design of precast RC structures: state of the art and construction practise in the Italian context," *Proceedings of the 2nd fib Congress*, Naples, Italy.
- [8] Calvi, G.M., Filippetto, M., Bolognini, D., Nascimbene, R. [2009] "Seismic design and retrofit of traditional Italian RC precast structures," *Proceedings of the Thematic Conference on Computational Methods*, Crete, Greece.
- [9] Ferrini, M., Lucarelli, E., Baglione, M., Borsier, S., Bortone, G., Ginori, R., Mangone, F., Mannella, A., Martinelli, A., Milano, L., Ntibarikure, M.C., Pirisi, P., Spampinato, A., Tucci, G. [2007] "DOCUP Toscana 2000-2006 – Azione 2.8.3: "Riduzione del rischio sismico nelle aree produttive" – Esiti dell'indagine di primo livello," *Proceedings of the 12th Conference of Seismic Engineering in Italy*, Pisa, Italy (in Italian).
- [10] Decreto Ministeriale 3 marzo 1975 [1975] "Approvazione delle norme tecniche per le costruzioni in zone sismiche," (in Italian).
- [11] Decreto Ministeriale 16 gennaio 1996 [1996] "Norme tecniche per le costruzioni in zone sismiche," (in Italian).
- [12] Verderame, G. M., Stella, A., and Cosenza, E. [2001] "Mechanical properties of reinforcing steel adopted in R.C. structures in the age '60", *Proceedings of the 10th National ANIDIS Conference: Seismic Engineering in Italy*, Potenza-Matera, Italy, (in Italian).
- [13] Bal, I.E., Crowley, H., Pinho, R., Gulay, F.G. [2008] "Detailed assessment of structural characteristics of Turkish RC building stock for loss assessment models," *Soil Dynamics and Earthquake Engineering*, Vol. 28, No. 11, pp. 914-932.
- [14] Casotto, C. [2013] "Seismic Vulnerability of Italian RC Precast Industrial Buildings," MSc Thesis, ROSE Programme, UME School, IUSS Pavia, Italy.
- [15] European Organisation for Technical Approvals – EOTA [2001] "ETAG 001 Guideline for European technical approval of metal anchors for use in concrete, Annex C: Design methods".
- [16] Decreto Ministeriale 3 dicembre 1987 [1987] "Norme tecniche per la progettazione, esecuzione e collaudo delle costruzioni prefabbricate," (in Italian).
- [17] Magliulo, G., Capozzi, V., Fabbrocino, G., Manfredi, G. [2011] "Neoprene-concrete friction relationships for seismic assessment of existing precast buildings," *Engineering Structures*, Vol. 33, No. 2, pp. 532-538.
- [18] Scott, B.D., Park, R. and Priestley, M.J.N. [1982] "Stress-Strain Behavior of Concrete Confined by Overlapping Hoops at Low and High Strain Rates," *ACI Journal Proceedings*, Vo. 79, No. 3, pp. 13-27.
- [19] Menegotto M., Pinto P.E. [1973] "Method of analysis for cyclically loaded R.C. plane frames including changes in geometry and non-elastic behaviour of elements under combined normal force and bending," *Symposium on the Resistance and Ultimate Deformability of Structures Acted on by Well Defined Repeated Loads*, International Association for Bridge and Structural Engineering, Zurich, Switzerland, pp. 15-22.
- [20] Crowley, H., Pinho, R., Bommer, J.J. [2004] "A probabilistic displacement-based vulnerability assessment procedure for earthquake loss estimation," *Bulletin of Earthquake Engineering*, Vol. 2, No. 2, pp. 173-219.
- [21] Erberik, M. A. [2008] "Fragility-based assessment of typical mid-rise and low-rise RC buildings in Turkey," *Engineering Structures*, Vol. 30, No. 5, pp 1360-1374.
- [22] Akkar, S., Sucuoglu, H., Yakut, A. [2005] "Displacement-Based Fragility Functions for Low- and Mid-rise Ordinary Concrete Buildings," *Earthquake Spectra*, Vol. 21, No. 4, pp 901-927.
- [23] Deyanova, M., Pampanin, S., Nascimbene, R. [2014] "Assessment of single-storey precast concrete industrial buildings with hinged beam-column connections with and without dowels". *Proceedings of the 2<sup>nd</sup> European conference on earthquake engineering and seismology*, Istanbul, Turkey.

- [24] Priestley, M. J., Calvi, G. M., Kowalsky, M. J. [2007] “Displacement - Based Seismic Design of Structures”. Pavia, Italy: IUSS Press.
- [25] Haselton, C. B. [2006] “Assessing seismic collapse safety of modern reinforced concrete moment frame Buildings”. Dissertation, Stanford University.
- [26] Fischinger, M., Kramar, M., & Isakovic, T. [2008] “Cyclic response of slender RC columns typical of precast industrial buildings”. *Bulletin of Earthquake Engineering*, Vol 6, No 3, pp. 519-534.
- [27] Brunesi E, Nascimbene R, Bolognini D, Bellotti D. [2015] “Experimental investigation of the cyclic response of reinforced precast concrete framed structures”. *PCI Journal*, Vol 60, No. 2, pp. 57-79.
- [28] Kramer, S. L. [1996] “Geotechnical Earthquake Engineering”.
- [29] Stewart, J.P., Chiou, S.J., Bray, R.W., Graves, P., Somerville, G., Abrahamson, N.A. [2001] “Ground motion evaluation procedures for performance-based design,” PEER report 2001/09, Pacific Earthquake Engineering Research Center, University of California, Berkeley.
- [30] Bommer, J.J., Acevedo, A.B. [2004] “The use of real earthquake accelerograms as input to dynamic analysis,” *Journal of Earthquake Engineering*, Vol. 8, No. 1, pp. 43-91.
- [31] Iervolino, I., Chioccarelli, E., Convertito, V. [2011] “Engineering design earthquakes from multimodal hazard disaggregation,” *Soil Dynamics and Earthquake Engineering*, Vol. 31, No. 9, pp. 1212–1231.
- [32] Borzi, B., Di Capua, G. [2011] “Carta delle tipologie di sottosuolo in base alle categorie delle NTC08 per l’Italia (scala 1:100.000), vincolata a punti di controllo stratigrafici, geotecnici e geofisici, per elaborazioni di pericolosità sismica”, Internal Report, EUCENTRE- INGV, (in Italian).
- [33] Decreto Ministeriale 14 gennaio [2008] “Norme Tecniche per le Costruzioni,” (in Italian).
- [34] Watson-Lamprey, J., Abrahamson, N. [2006] “Selection of ground motion time series and limits on scaling,” *Soil Dynamics and Earthquake Engineering*, Vol. 26, No. 5, pp. 477–482.
- [35] Crowley, H., Colombi, M., Silva, V., Ahmad, N., Fardis, M., Tsionis, G., Papailia, A., Taucer, F., Hancilar, U., Yakut, A., Erberik, M.A. [2011] “Fragility functions for common RC building types in Europe,” *Systemic Seismic Vulnerability and Risk Analysis for Buildings, Lifeline Networks and Infrastructures Safety Gain Project*, Deliverable 3.1. Available from URL: [www.vce.at/SYNER-G/files/dissemination/deliverables.html](http://www.vce.at/SYNER-G/files/dissemination/deliverables.html)
- [36] Silva, V., Crowley, H., Varum, H., Pinho, R. [2014] “Investigation of the characteristics of Portuguese regular moment-frame RC buildings and development of a vulnerability model”. *Bulletin of Earthquake Engineering*, in press, DOI 10.1007/s10518-014-9669-y.
- [37] Vamvatsikos, D., Cornell, A. [2005] “Developing efficient scalar and vector intensity measures for IDA capacity estimation by incorporating elastic spectral shape information,” *Earthquake Engineering and Structural Dynamics*. Vol. 34, No. 13, pp. 1573–1600.
- [38] Baker J.W. and Jayaram N. [2008] “Correlation of spectral acceleration values from NGA ground motion models,” *Earthquake Spectra*, Vol. 24, No. 1, pp. 299-317.
- [39] Beyer, K., and Bommer, J. J. [2006] “Relationships between median values and between aleatory variabilities for different definitions of the horizontal component of motion,” *Bull. Seism. Soc. Am.*, Vol. 96, No. 4A, pp. 1512–1522.
- [40] Minghini, F., Ongaretto, E., Ligabue, V., Savoia, M., Tullini, N. [2014] “Un primo inventario dei danni in edifici prefabbricati a seguito del sisma dell’Emilia del 2012,” *Proceedings of the 20<sup>th</sup> conference of the Collegio dei Tecnici della industrializzazione Edilizia (CTE)*, Milan, Italy, (in Italian).

#### Web References:

- [1] OpenSEES: <http://opensees.berkeley.edu/>
- [2] Matlab: <http://www.mathworks.com/>
- [3] Tuscany Region: <http://www.regione.toscana.it>
- [4] EUCENTRE: <http://www.eucentre.it>
- [5] SeismoStruct <http://www.seismosoft.com>
- [6] PEER strong motion database: <http://peer.berkeley.edu/smcat/>